JACS
JOURNAL OF THE AMERICAN CHEMICAL SOCIETY

ARTICLE

pubs.acs.org/JACS

Molecular Hydrogen Tweezers: Structure and Mechanisms by Neutron Diffraction, NMR, and Deuterium Labeling Studies in Solid and Solution

Felix Schulz,[†] Victor Sumerin,[‡] Sami Heikkinen,[‡] Björn Pedersen,[§] Cong Wang,[‡] Michiko Atsumi,[∥] Markku Leskelä,[‡] Timo Repo,*[,‡] Pekka Pyykkö,[‡] Winfried Petry,[§] and Bernhard Rieger*[,†]

[†]WACKER-Lehrstuhl für Makromolekulare Chemie and [§]Forschungs-Neutronenquelle Heinz Maier-Leibnitz, Technische Universität München, Lichtenbergstrasse 4, D-85747 Garching bei München, Germany

[‡]Department of Chemistry, University of Helsinki, P.O. Box 55, FIN-00014 Helsinki, Finland

[∥]Department of Physical and Analytical Chemistry, Quantum Chemistry, Uppsala University, P.O. Box 518, SE-75120 Uppsala, Sweden

Supporting Information

ABSTRACT: The mechanism of reversible hydrogen activation by *ansa*-aminoboranes, 1-*N*-TMPH-CH_2-2-[$HB(C_6F_5)_2$]C_6H_4 (**NHHB**), was studied by neutron diffraction and thermogravimetric mass-spectroscopic experiments in the solid state as well as with NMR and FT-IR spectroscopy in solution. The structure of the *ansa*-ammonium borate **NHHB** was determined by neutron scattering, revealing a short N−H···H−B dihydrogen bond of 1.67 Å. Moreover, this intramolecular H−H distance was determined in solution to be also 1.6−1.8 Å by ^{1}H NMR spectroscopic T_1 relaxation and 1D NOE measurements. The X-ray B−H and N−H distances deviated from the neutron and the calculated values. The dynamic nature of the molecular tweezers in solution was additionally studied by multinuclear and variable-temperature NMR spectroscopy. We synthesized stable, individual isotopic isomers **NDDB**, **NHDB**, and **NDHB**. NMR measurements revealed a primary isotope effect in the chemical shift difference $^P\Delta^1H(D) = \delta(NH) - \delta(ND)$ (0.56 ppm), and hence supported dihydrogen bonding. The NMR studies gave strong evidence that the structure of **NHHB** in solution is similar to that in the solid state. This is corroborated by IR studies providing clear evidence for the dynamic nature of the intramolecular dihydrogen bonding at room temperature. Interestingly, no kinetic isotope effect was detected for the activation of deuterium hydride by the *ansa*-aminoborane **NB**. Theoretical calculations attribute this to an "early transition state". Moreover, 2D NOESY NMR measurements support fast intermolecular proton exchange in aprotic CD_2Cl_2 and C_6D_6.

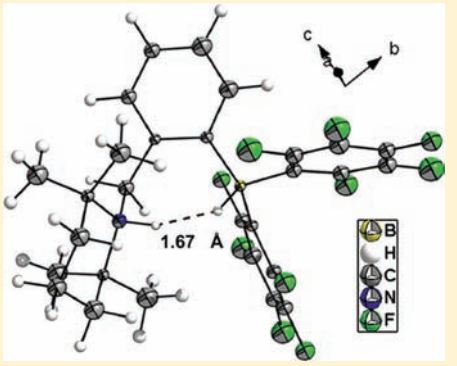

INTRODUCTION

Although, or maybe because, dihydrogen is the simplest existing nonpolar molecule, it is one of the most important ones in industry. Catalytic hydrogenation reactions are among the most massive man-made chemical reactions in the world. The hydrocracking of crude oil, the Haber-Bosch process for ammonia synthesis, and the Fischer−Tropsch process, which is gaining in importance lately due to rising oil prices, are just a few examples.[1] Moreover, hydrogen is also employed in the manufacturing of polyolefins and a vast variety of base chemicals like methanol, cyclohexane, and aniline and in the hardening of oils and fats, and it is essential for the synthesis of many specialty chemicals and pharmaceuticals, especially in the form of asymmetric hydrogenations.[2] In these processes the activation of the dihydrogen molecule is most often achieved by a transition-metal center in homogeneous, heterogeneous, or biological catalysts.[3] Because of this importance of hydrogenation reactions, even minor improvements can lead to substantial monetary savings. In order to achieve this, a good understanding of the mechanistic details is indispensable. Therefore, the splitting of H_2 has received intensive interest from numerous researchers.[4] The discoveries of nonclassical H_2 complexes by Kubas et al.,[5] and of dihydrogen bonds by Crabtree, Siegbahn, and co-workers,[6] are important milestones in this area.

The recently developed class of nonmetal compounds, called "frustrated Lewis pairs" (FLPs), have received a great amount of interest. They have been shown to activate dihydrogen and other small molecules.[7] In most cases the release of hydrogen gas from corresponding onium boron hydrides is not thermodynamically favored. If the reaction is almost thermodynamically neutral, the inverse reaction, a facile hydrogen liberation, can take place under mild conditions. Thus, some of the reported FLP systems were shown to reversibly activate hydrogen[8−10] and, more recently, to act as efficient metal-free hydrogenation catalysts.[11−13] Since a complete absence of transition metals is required in pharmaceutical products, due to toxicity concerns, FLPs are a very attractive

Received: July 10, 2011
Published: November 16, 2011

dx.doi.org/10.1021/ja206394w | *J. Am. Chem. Soc.* 2011, 133, 20245–20257

Chart 1. Molecular Structure of the *ansa*-Ammonium Borates NHHB (X = Y = H), NDDB (X = Y = D), NDHB (X = D, Y = H), and NHDB (X = H, Y = D)

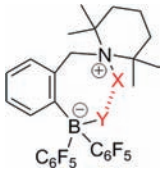

alternative to conventional hydrogenation catalysts currently applied in the pharmaceutical industry.[14] With the help of FLPs even asymmetric hydrogenations are achievable.[15,16]

For further development of improved FLP-based catalysts, knowledge of the mechanistic and structural details of these systems is of utmost importance. Many research groups have studied the mechanistic aspects of hydrogen activation by FLPs theoretically before.[17] In particular the initial step has been discussed.[18,19] Some structural features, like the prearrangement of fluorine-containing FLPs in solution due to N−H···F or C−H···F bonds, are also suggested by experiments.[20]

In a recent theoretical study on hydrogen activation by various previously reported FLPs, Rokob et al. concluded that the reaction has to be slightly exergonic at standard conditions so that the reverse reaction is also feasible.[8] **NHHB** (Chart 1) is one of the few nitrogen-based systems that can release the bound hydrogen in solution upon heating, but the computed Gibbs free energy was too low, pointing at an at least partly incorrect description by the applied theoretical methods.[11] Despite the indication that it also contains one of the shortest N−H···H−B dihydrogen bonds reported so far in the literature, its exact length could not be obtained by X-ray diffraction due to the poor visibility of H-atoms by this method. In order to clarify this, we were motivated to carry out a neutron diffraction study on **NHHB**.

To the best of our knowledge, the FLP systems based on the *ansa*-ammonium borate concept have also the highest catalytic activity among previously reported organocatalytic systems for a wide range of nitrogen-containing substrates.[13,16,21] We furthermore elucidated the solution structure and the hydrogen exchange mechanisms by ^{1}H NMR T_1 relaxation measurements, selective deuterium−hydrogen exchange, and characterization of the hydron-loaded[22] compounds (Chart 1) by multinuclear NMR, selective 1D NOE measurements, 2D NOESY NMR, IR spectroscopy and high-resolution ESI-TOF (HRESI-TOF),[23] variable-temperature (VT) ^{1}H, ^{11}B NMR and VT FIR/MIR solution-state experiments, and TG-MS of the solids.

RESULTS AND DISCUSSION

NMR Studies. The new NMR spectra of **NHHB** recorded in CD_2Cl_2 essentially do not differ from the previously reported spectra measured from C_6D_6 solutions.[11] The ^{1}H NMR spectrum of **NHHB** in CD_2Cl_2 shows the broad quartet at 3.76 ppm with a coupling constant of 77 Hz ($^1J_{HB}$), characteristic for the B*H* hydride and corresponding to the splitting observed in the doublet at −20.84 ppm in ^{11}B NMR data. The chemical shift difference between the fluorine signals ($\Delta\delta_{p,m}$ = 3.40 ppm) in ^{19}F NMR provides further evidence for an anionic four-coordinate borate.[24] In the ^{1}H NMR data, the broad singlet[25] ($\Delta\nu_{1/2}$ = 165 Hz) at 7.77 ppm is assigned to the N*H* proton (Figure 1a). The broadness of the signal can be attributed to a combination of proton exchange

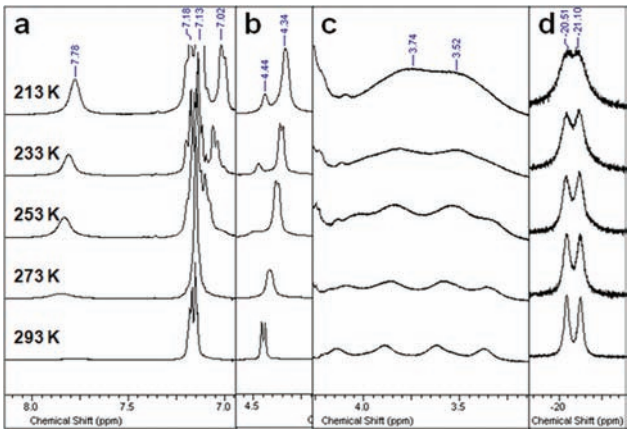

Figure 1. 300 MHz VT NMR spectra of **NHHB** in CD_2Cl_2: (a) N*H* (around 7.8 ppm) and C_6H_4 (around 7.1 ppm) ^{1}H NMR signals; (b) CH_2 ^{1}H NMR signals; (c) B*H* ^{1}H NMR signals; (d) ^{11}B NMR signals.

and quadrupolar relaxation effects of the neighboring ^{14}N nucleus.[26] The signal is slightly shifted downfield (0.22 ppm), compared to the chemical shift observed in C_6D_6. This can be ascribed to the different polarities of the solvents. Unfortunately, no $^1J_{HH}$ coupling across the dihydrogen bond is visible in either N*H* or B*H* resonances due to the broad line widths.[27] The doublet at 4.45 ppm can be assigned to the benzylic CH_2 bridging the phenyl ring to the 2,2,6,6-tetramethylpiperidine (TMP). The observed coupling, $^3J_{HH}$ = 5.5 Hz, originates from coupling to the N*H*. This was readily confirmed by disappearance of the aforementioned splitting from the benzylic CH_2 signal with the **NDHB** sample (see below).

In Figure 1b the CH_2 signal is shown to split into one large signal approximately at 4.34 ppm and one small signal at 4.44 ppm, which could be caused by dynamic equilibria between two tautomers or two conformers. In the case of a dynamic equilibrium within the dihydrogen bond, the proton can take up two different positions between the nitrogen and the hydride (H8)[28] within the molecule: one relatively close to N and far away from H8, and the second position the other way around (far from N and so close to H8 that a side-on-bound H_2 complex forms). This can be compared to the tautomerism found in systems containing intramolecular hydrogen bonds (Scheme 1). For conformational isomerism, two structures, which convert into each other through ring-inversion of the piperidine moiety, are presented in Scheme 2: **NHHB(1)** is identical with the solid-state structure. It is not unreasonable to assume that it is also the most stable one in solution. Hints to the existence of its conformational isomer **NHHB(2)** were recently found by us when studying similar compounds where TMP was replaced by a 2,2,4-trimethyl-1,2,3,4-tetrahydroquinoline moiety.[16] In a study performed by Berke and co-workers, a similar conformational equilibrium was found in the piperidinium borate $[TMPH]^+[HB(C_6F_5)_3]^-$.[29]

In VT NMR studies the coupling of the CH_2 signals cannot be observed at lower temperatures, but this is most probably caused by a slower rotation, resulting in line broadening. The ratio between the two CH_2 signals was estimated to be on the order of 9:1, which would also be the ratio of the corresponding rate constants. As pointed out before, conformer **NHHB(1)** is the more stable one, and hence $k_1 > k_2$. At the same time, additional signals appear for the hydrogen atoms attached to the piperidine ring upon lowering of the temperature.[23] It is therefore believed that two conformational isomers exist, as shown in Scheme 2.

Scheme 1. Possible Tautomerism of NHHB in Solution

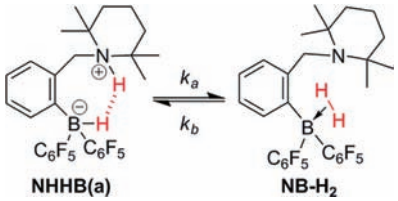

Scheme 2. Schematic Equilibrium between Two Conformational Isomers of NHHB in Solution

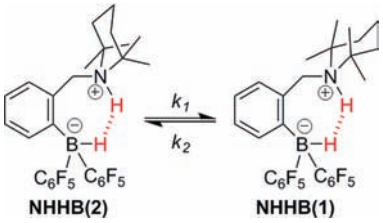

The B*H* signal in Figure 1c is not shifted, but the shape of the quartet is not resolved any more at low temperature. This is also an effect of line broadening which could be caused by less rotational freedom and faster relaxation. The corresponding effect can be observed in the ^{11}B NMR spectrum, too (Figure 1d). The nicely resolved doublet becomes broader with decreasing temperature, but does not change otherwise. In addition, this is the only signal that can be detected. Therefore, the environment of ^{11}B and H8 does not seem to change dramatically with the conversion of **NHHB(1)** to **NHHB(2)**.

The deuterated *ansa*-ammonium borate **NDDB** was synthesized by analogy to **NHHB**: A yellow solution of **NB** in pentane reacted rapidly with D_2 at room temperature to give a white suspension of **NDDB** in quantitative yield (Scheme 3). At 110 °C a solution of **NDDB** in toluene turned yellow again like the *ansa*-ammonium borate **NHHB**, indicating that **NB** can reversibly activate D_2 just like H_2.

By comparison of the spectroscopic data for **NDDB** and **NHHB** the following observations can be made: the ^{19}F NMR spectra are identical ($\Delta\delta_{p,m}$ = 3.40 ppm); the ^{11}B resonance shows a singlet at −21.07 ppm instead of a doublet; the ^{1}H spectra are to a large extent identical with the exceptions that the broad quartet at 3.76 ppm and the broad singlet at 7.77 ppm are absent, and the C*H*$_2$ signal at 4.44 ppm is a singlet instead of a doublet. These data are perfectly in line with the formulation of **NDDB** as the only product. In this case, the small couplings to deuterons were not resolved because the couplings are smaller ($J_{HD} \approx J_{HH}/6.5$), and the quadrupolar D may have faster relaxation.[30]

The ^{2}H NMR spectrum shows the N*D* and B*D* resonances as broad singlets[25] at 7.21 and 3.76 ppm, respectively. The latter of the two should appear as a quartet due to the coupling to the ^{11}B nucleus, but the coupling constant seems to be too small with respect to the line width to allow the detection of the fine structure. The N*D* signal is shifted upfield by 0.56 ppm in comparison to the corresponding signal of **NHHB** in the ^{1}H NMR spectrum. The difference in chemical shift $^{p}\Delta^{1}H(D) = \delta(NH) - \delta(ND)$ between the two hydrons is called a primary isotope effect. It is now positive and quite large. When comparing it to literature, such a value would indicate the existence of a strong H-bond, as outlined by Dziembowska and Rozwadowski in detail—herein a strong dihydrogen bond—in **NHHB**.[31] Equilibrium and intrinsic isotope effects on chemical shifts have been discussed in the literature. The first arise from different zero-point energies (ZPEs) in the different states of the equilibrium and the second from geometric isotope effects arising from anharmonic ground isotopic vibrations.[32]

Scheme 3. Reversible D_2 Activation by the System NB/NDDB

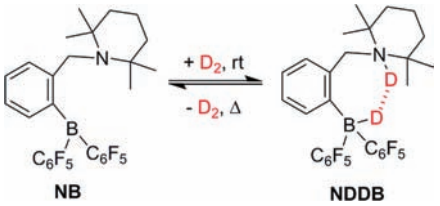

At first we concluded that the large value of the isotope effect might indicate the existence of a double-well potential and thus tautomerism within the system **NXYB** (X, Y = H or D) in solution (Scheme 1), but it has been shown that all the above-mentioned effects contribute to the observed values.[33] Therefore, the reported effects do not indicate the presence of tautomerism. If such a tautomerism existed then the inter-hydron distance in **NB-H$_2$** would be so small that a side-on-bound H_2 complex would be likely.[34] Such a structure would imply a rapid exchange between the two hydrons caused by classic and quantum mechanical exchange.[35] This in turn would result in a coalescence of the N*H* and B*H* signals which in fact is not observed. Therefore, a tautomerism as shown in Scheme 1 and hence also a double-well potential can be excluded.

Literature reports on such isotope effects regarding dihydrogen bonding were not found; only the more common hydrogen bonds to O, N, and S have been previously studied in detail.[36] We therefore performed VT ^{1}H NMR studies of **NHHB** in C_6D_5Br between 253 and 356 K and VT ^{2}H NMR studies of the products of HD splitting by **NB** in CH_2Cl_2 between 213 and 293 K.[23] It can clearly be seen that the N*H* signal of **NHHB** shifts to higher field upon increasing the temperature, even though the peak cannot be clearly seen due to overlapping aromatic signals. At the same time, the N*D* signal shifts to lower field upon decreasing the temperature. The magnitude of the observed chemical shift change is in both cases around 0.5 ppm. This suggests two possible structures of the NH and the ND moiety, respectively: high- and low-temperature structures. Due to different binding strengths of H and D, the change between the structures happens at different temperatures in both cases. The structure of NH changes between 293 and 316 K, and the structure of ND changes between 243 and 273 K. It is thought that the two structures might be caused by weak NH−solvent interactions. The change of N*H*/N*D* chemical shifts in altered measurement temperatures follows well-documented behavior for common hydrogen-bonding groups (water, alcohols, amines, etc).[37] The shift of X to lower field suggests more pronounced bonding of X with N, i.e., a shorter N−X distance at lower temperatures which allows X to share its electrons with N more efficiently, leading to a deshielding of X. The shift to higher field at elevated temperatures is caused by weaker N−X bonding, possibly

dx.doi.org/10.1021/ja206394w |J. Am. Chem. Soc. 2011, 133, 20245–20257

arising from an increased N−X distance, and therefore increased electron density on X.

H−D Exchange in Solution. When **NHHB** is dissolved in a methanol-d_1/benzene mixture (40/60) at room temperature, an H−D exchange takes place immediately. By removal of the solvent and addition of fresh CH_3OD for a second time, **NHHB** is converted completely into **NDHB**. Protic solvents lead in the same way to the back-conversion of **NDHB** into **NHHB**.

The ^{1}H NMR spectrum of **NDHB** in CD_2Cl_2 exhibits a broad quartet[25] at δ = 3.72 ppm with a coupling constant of $^1J_{HB}$= 76 Hz showing the existence of the B*H* hydride, as documented before for **NHHB**. The broad singlet of the protic N*H* is missing, but all other signals stay put. The CH_2 resonance at 4.44 ppm is a singlet due to the small coupling constant of N*D*. The ^{11}B NMR signal at −20.86 ppm (doublet, $^1J_{BH}$ = 77 Hz) and the chemical shift difference of F atoms ($\Delta\delta_{p,m}$ = 3.40 ppm) are consistent with a four-coordinate anionic boron.[24] It can be concluded that the steric and electronic structures of the molecule do not change dramatically. At the same time a broad singlet[25] at 7.20 ppm can be observed in a ^{2}H NMR spectrum as the only signal which is assigned to N*D*. The primary isotope effect exists in this molecule, too, and it is of the same size (0.57 ppm) as in **NDDB**.

Upon warming of a colorless solution of **NDHB** in toluene-d_8 up to 60 °C for several hours and subsequent cooling, the molecule stays intact. Formation of **NHDB** did not take place, as evidenced by multiple-nucleus NMR spectra, implying that no rotation of D···H occurred. In a very recent publication, Piers et al. observed the same for the ion pair $[^tBu_3PH]^+[DB(C_6F_5)_3]^-$ dissolved in C_6D_5Br up to 100 °C.[19] Above 65 °C the solution started to turn slightly yellow and signals for **NB** could be detected in NMR spectra. The exchangeability seems to be restricted to the N-bound hydron, whereas the B-bound hydron always remains in the same place until **NB** is formed. This is another direct experimental proof that **NB-H$_2$** and hence the tautomerism depicted in Scheme 1 cannot exist.

In order to synthesize **NHDB**, a procedure similar to that used for **NDHB** was applied. This time **NDDB** was used as the starting compound, which was dissolved in a mixture of methanol/benzene (40/60) at room temperature. After stirring, evaporation of solvents, and repeating these steps once, **NHDB** was obtained as a white solid in near-quantitative yield.

The N*H* resonance is detected at 7.70 ppm as a broad singlet[25] in the proton NMR spectrum, and the CH_2 group causes a doublet at 4.44 ppm ($^3J_{HH}$ = 6 Hz) as observed in the corresponding spectrum of **NHHB**. No broad quartet appears around 3.8 ppm, but instead a broad singlet[25] shows up at 3.80 ppm in the ^{2}H NMR spectrum which is in line with a B*D* fragment. Additionally, the ^{11}B spectrum shows a singlet at −21.15 ppm, and the chemical shift difference of F atoms is $\Delta\delta_{p,m}$ = 3.39 ppm, indicating a four-coordinate anionic borate.[24] **NHDB** behaves in the same way as **NDHB**: only the N-hydron can be exchanged easily in solution, but no rotation of H−D can be observed at elevated temperatures before **NB** is formed.

Reaction of NB with HD. Reacting HD gas at room temperature with a yellowish pentane **NB** solution, a white precipitate forms within minutes. By multinuclear NMR, FT-IR, or HRESI-TOF MS analysis methods, it could not be determined whether only **NHDB** and **NDHB**, or all four possible isomers (**NHHB**, **NHDB**, **NDHB**, **NDDB**), formed. Therefore, additional 2D NOESY NMR studies of pure **NHHB**, used as a standard, and this reaction mixture were performed. Spectra were recorded first in CD_2Cl_2 and later in C_6D_6 (see the Experimental Section for further details). The N*H*−*H*B cross-peak volumes of both experiments gave evidence for the existence of all four isomers (Figure 2).[38] Consequently, control experiments of separately synthesized equimolar solutions of **NHDB** and **NDHB** were performed. After an equilibration time of several hours in CD_2Cl_2, the recorded 2D (H,H) NOESY spectrum showed an N*H*−*H*B cross-peak volume that can be ascribed to an approximately 0.25:0.25:0.25:0.25 mixture of all four possible isotopomers **NHHB**, **NHDB**, **NDHB**, and **NDDB**, demonstrating an intermolecular proton exchange. The same measurement was performed, applying the dry aprotic and apolar C_6D_6 as solvent, and again the spectrum gave evidence for the existence of all four isotopomers with approximate ratios of 0.15:0.35:0.35:0.15; i.e., the exchange is less complete than in CD_2Cl_2.[23]

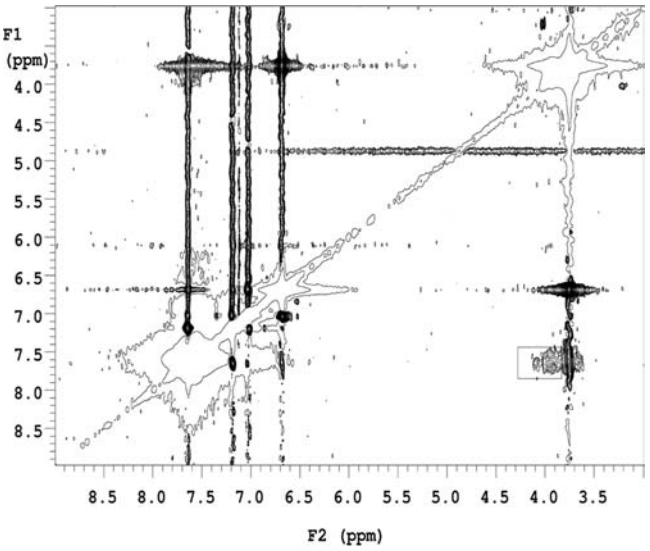

Figure 2. Expansion of the NOESY spectrum (500 MHz, 600 ms mixing time) recorded from a C_6D_6 sample of **NB** reacted with HD. Negative peaks (diagonal) are given by two sparsely placed contours. Positive signals are depicted by several densely spaced contours. The rectangle centered at 4.00, 7.70 ppm (f_2, f_1) shows the limits for 2D integration to determine the N*H*−*H*B correlation peak volume. Effectively, only half of the cross-peak volume is captured, and the data have to be multiplied by 2 to estimate the actual N*H*−*H*B NOESY cross-peak volume.

As discussed before, careful sample preparation ensured that only traces of water can be expected in them, rendering significant contributions of N*H* exchange between residual water impossible. On the other hand, minuscule amounts of water (μg/mL range) cannot be ruled out, and water molecules could act as proton carriers, enabling a proton exchange between two molecules of **NXYB** through H_2O. Another possible mechanism could be that protons migrate via the free-electron pairs of the fluorine atoms (or chlorine in the case of CD_2Cl_2 as solvent). The hydrons could not be directly exchanged between two ammonium groups because of missing free-electron pairs.

In conclusion, the fast intermolecular proton exchange prevents the unambiguous proof of an intramolecular mechanism of hydrogen splitting by **NB**. Nevertheless, additional experiments show that the very strong Lewis acid $B(C_6F_5)_3$ remains unchanged during H_2 activation by **NB**.[23] This and theoretical calculations support intramolecular hydrogen activation.[11] After splitting of the hydrogen, the proton exchange can take place with the help of trace amounts of water, as suggested here.

Scheme 4. Possible Transition States during Hydrogen Activation by NB

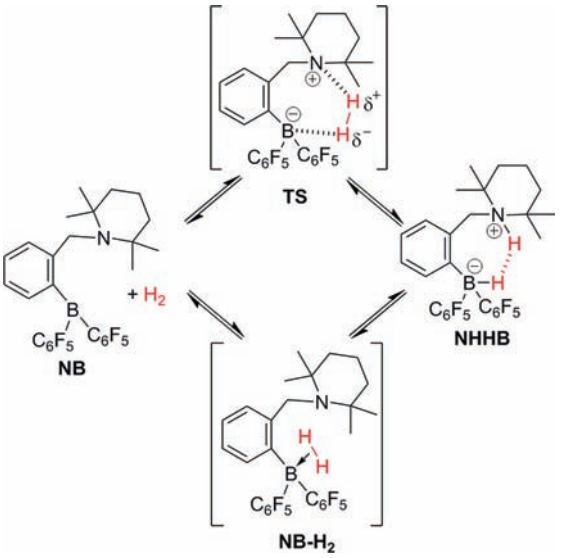

At the same time, the ^1H and ^2H NMR data of the reaction products of **NB** and HD in solution exhibited a ratio between N-bound H (or D) and B-bound H (or D) atoms of 1:1. Thus, no kinetic isotope effect (KIE) can be observed, which is not surprising because in the theoretical calculation of the H_2 splitting by **NB** an early transition state (**TS** in Scheme 4) is found in a concerted mechanism.[11] In this structure the H_2 bond is only slightly elongated and the B−H and N−H bonds are formed simultaneously.

The formation of an η^2-bound adduct between **NB** and dihydrogen (**NB-H$_2$** in Scheme 4) on the other hand could explain the absence of a KIE, too. H_2 binding to the Lewis acidic boron center would then be the rate-limiting step before the fast intramolecular deprotonation of the adduct by the Lewis basic nitrogen takes place to form **NHHB**. We did search for an η^2 H_2 transition state, but could not find any for **NB** in our calculations. In addition we did not observe any rotation of H−D in heated solutions of **NHDB** and **NDHB**. Experimental evidence for **NB-H$_2$** is therefore also missing.

This is in contrast to the findings of Fan et al., who favored the pathway of FLP-assisted side-on dihydrogen activation, similar to transition metal-H_2 σ bond complexes.[18] Gao et al. reported an intermediate on the proton-transfer pathway, consisting of an H_2 σ bond complex $(CF_3)_3B(\eta^2\text{-}H_2)\cdots PH_3$.[39] They also emphasized the dihydrogen bond aspect of the loaded B−H···H−P complex. The conceptually related mechanism of the $B(C_6F_5)_3$-catalyzed hydrosilylation of various functions, which involves a borane−silane adduct during activation, is already well-established.[40]

According to Table 1, the ZPE and Gibbs free energy isotopic differences are quite small at **TS**, although they become larger for the products. This supports the idea that the early transition state does not produce an isotope effect (Figure 3). In their study of phosphorus−boron-based FLP systems, Grimme et al.[17h] emphasized the role of ligand−ligand attractions from dispersion and found a barrier, or transition state, for one of their systems. It was an "early" one, like ours. They also suggested replacing the entire host molecule (here **NB**) by a strong electric field, an even stronger theoretical simplification than the "Coulomb pays for

Table 1. Reaction Energies of NB + HD → NHDB and NDHB from CAM-B3LYP/6-31G Calculations (in kJ/mol)[a]**

	Transition States			
	$\Delta^{\ddagger}E$	$\Delta^{\ddagger}E$ + ZPE	$\Delta^{\ddagger}H$	$\Delta^{\ddagger}G$
NHDB	21.08	33.41	25.93	68.07
NDHB	21.08	33.39	25.90	68.01
NHHB	21.08	31.37	27.50	68.54
NDDB	21.08	35.65	24.49	67.66
	Products			
	ΔE	ΔE + ZPE	ΔH	ΔG
NHDB	−89.52	−56.24	−64.40	−22.66
NDHB	−89.52	−58.78	−66.45	−24.57
NHHB	−89.52	−52.29	−60.27	−20.25
NDDB	−89.52	−62.00	−69.92	−26.45

[a] The corresponding data of **NHHB** and **NDDB** are included for comparison. $\Delta^{\ddagger}$ and Δ denote the activation and reaction energies. *E*, *E* + ZPE, *H*, and *G* correspond to electronic energy, electronic + zero point energy, enthalpy, and Gibbs free energy at 298.15 K and 1 atm, respectively. The computed rate constant ratio results in $k_{NHDB}/k_{NDHB} = 0.98$.

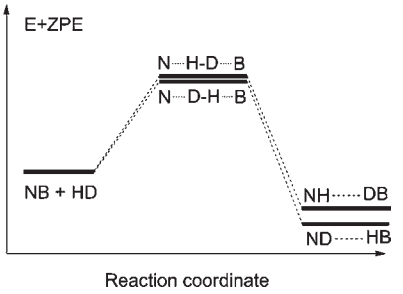

Figure 3. Zero-point energies of starting compounds, transition states, and products along the pathway of the reaction of **NB** with deuterium hydride assuming an intramolecular mechanism.

Heitler-London" one.[11] There it meant that the attraction between the resulting counterions is comparable with the splitting energy for H_2. With more than one ion pair, a "collective Madelung ionization" can result.[17g]

Neutron Diffraction. We previously reported the crystal structure of **NHHB** determined by X-ray diffraction.[11] In addition, we performed density functional theory (DFT) calculations at the PBE/6-31G(d) level of theory for geometry optimizations, and the reaction path, utilizing the PCM method to account for solvation effects. Rokob et al. also optimized the geometry of this *ansa*-ammonium borate, but only in the gas phase using DFT at the M05-2X/6-31G(d) level.[8] The geometries determined by these different methods were in good agreement overall but varied significantly in the value for the soft intramolecular N−H···H−B dihydrogen bond distance (Table 2). Unfortunately this is the part of main interest within this molecule since these two hydrogen atoms can either be released as dihydrogen gas which can then be split up again by the resulting **NB** or transferred to other molecules like imines, enamines, and nitrogen-containing heterocycles. In order to determine precisely the actual geometry of **NHHB** we conducted a neutron diffraction

dx.doi.org/10.1021/ja206394w |J. Am. Chem. Soc. 2011, 133, 20245–20257

Table 2. Comparison of Structural Data of NHHB Obtained by Different Methods: Single-Crystal Neutron Diffraction, Single-Crystal X-ray Diffraction, ab Initio Geometry Optimization in Solution at the PBE/6-31G(d) Level of Theory Utilizing the PCM Model, and ab Initio Geometry Optimization in the Gas Phase at the M05-2X/6-31G(d) Level (The Presented Data Describe the N−H···H−B Moiety)

property	ND	XRD[a]	PBE/ 6-31G(d)[a]	M05-2X/ 6-31G(d)[b]
d(H−H) [Å]	1.67	1.78	1.51	1.53
d(N−H) [Å]	1.03	0.94	1.06	1.04
d(B−H) [Å]	1.24	1.19	1.24	1.23
d(N−B) [Å]	3.35	3.36	3.34	3.25
ψ(∠N−H···H) [deg]	154.9	154.2	150.3	159.7
θ(∠B−H···H) [deg]	123.1	125.2	132.5	122.9

[a] Data taken from ref 11. [b] Data taken from ref 8.

measurement on a single crystal grown out of a C_6D_6 solution by slow cooling of a supersaturated solution.

The crystals were determined to be triclinic and could be refined to yield the structure reported in Figure 8 unambiguously. Good R values of 0.066 ($R1$) and 0.065 (w$R2$) could be reached, and further refinement was impossible, mainly due to disordered solvent molecules. It is well-known that N−H and B−H bond lengths are underestimated when determined by X-ray diffraction.[41,42] Both the calculated and the neutron values are clearly larger, and mutually agree. The N−H bond length of **NHHB** (1.03 Å) fits well the one in the stable Lewis acid/Lewis base adduct $H_3N{\cdot}BH_3$, determined previously by a neutron diffraction study to be 1.03 Å, which is a widely accepted standard value for N−H bonds.[6,43] The B−H bond of 1.17 Å in the $H_3N{\cdot}BH_3$ weak complex is shorter. Further neutron values for B−H and B−D bonds are 1.21 Å.[6,43,44] Thus, the B−H bond in **NHHB** (1.24 Å) is only very slightly elongated. The actual dihydrogen bond length of only 1.67 Å is one of the smallest values reported in literature so far for N−H···H−B compounds.[45] For comparison, the so-called van der Waals radii of both hydrogen atoms sum up to 2.4 Å. The sum of the van der Waals radii is a measure on the strength of dihydrogen bonds.[46] It is therefore assumed that in the close H···H contact within **NHHB** the dihydrogen bond is comparatively strong and partly covalent in nature.[47] Additionally, the bonding angles ψ and θ (see Table 2) also agree well with previously reported structures containing N−H···H−B dihydrogen bonds.[6,45]

H1···H8 Interproton Distance Determinations in Solution Applying T_1 Relaxation Measurements and Selective 1D NOE Experiments. Having determined the precise structure of **NHHB** in the solid state, we were curious about its structure in solution, since this is the surrounding where the system actually activates, transfers, and liberates hydrogen. Therefore we conducted T_1 relaxation measurements by ^{1}H NMR spectroscopy of the activated dihydrogen within **NHHB** in CD_2Cl_2 solution. According to eq 1, the relaxation rate $1/T_1$(H−H) of one proton due to dipole−dipole interaction with another proton depends on the interatomic proton−proton distance r_{H-H}. The symbols γ, $\hbar$, τ_c, and ω represent gyromagnetic ratio, Planck's constant/2π, correlation time, and Larmor frequency, respectively. Application of minimum relaxation times T_1(min) allows the use of eq 2 and hence a single correlation time τ_c. The determined T_1(min) values are rather short as expected for close H···H contacts: 44.8 ms for B−H ($T_1(\mathrm{min})_{H1}$) and 92.1 ms for N−H ($T_1(\mathrm{min})_{H8}$) at 213 K and 300 MHz. As can be seen from eq 3, the measured relaxation rate $1/T_1$(H) is the sum of relaxation rates based on dipole−dipole interactions with all protons H_i and other NMR-active nuclei X in close proximity to H. Because both H-atoms (H1/H8) are additionally in close contact to other nuclei, which contribute to a large extent to the fast relaxation (especially B, F, N, and other H-atoms), the original T_1 criterion as defined by Crabtree and Hamilton is not valid.[48] Instead, the enhanced approach by Halpern and co-workers was utilized to determine the H···H distance in solution. Therefore, eqs 1 and 4 were applied to determine the single contributions from dipole−dipole relaxation to the observed relaxation rates $1/T_1(\mathrm{min})_{H1}$ and $1/T_1(\mathrm{min})_{H8}$. The distances (r_{H-H}, r_{H-X}) between H1/H8 and other nuclei reported in the Supporting Information were taken from the measured neutron diffraction structure.[49] Additionally the natural abundances of the different nuclei were also taken into account.

$$\frac{1}{T_1(\mathrm{H-H})} = \frac{3}{10}\frac{\gamma_H^4\hbar^2}{r_{H-H}^6}\left[\frac{\tau_c}{1+\omega_H^2\tau_c^2}+\frac{4\tau_c}{1+4\omega_H^2\tau_c^2}\right] \quad (1)$$

$$\tau_c = \frac{0.6158}{\omega} \quad (2)$$

$$\frac{1}{T_1(\mathrm{H})} = \sum_i \frac{1}{T_1(\mathrm{H-H}_i)} + \sum_X \frac{1}{T_1(\mathrm{H-X})} \quad (3)$$

$$\frac{1}{T_1(\mathrm{H-X})} = \frac{2}{15}\frac{\gamma_H^2\gamma_X^2\hbar^2}{r_{H-X}^6} I(I+1) \times \left[\frac{3\tau_c}{1+\omega_H^2\tau_c^2}+\frac{6\tau_c}{1+(\omega_H+\omega_X)^2\tau_c^2}+\frac{\tau_c}{1+(\omega_H-\omega_X)^2\tau_c^2}\right] \quad (4)$$

These values were then used to solve eq 3 to get $1/T_1(\mathrm{min})_{H1-H8}$ and $1/T_1(\mathrm{min})_{H8-H1}$. Therefore two independent values for the H1···H8 distance resulted out of the calculation based on the different T_1(min) values: $T_1(\mathrm{min})_{H1}$ led to 1.72 Å and $T_1(\mathrm{min})_{H8}$ to 1.69 Å.

In addition, 300 MHz T_1 data were also analyzed by fitting a theoretical T_1 curve to the measured T_1 values of both nuclei H1 and H8. The fitted curve includes all relaxation contributions from other nuclei (i.e., based on distances obtained from the neutron diffraction structure). The full treatment of T_1 curves of H1 and H8 resulted in H1···H8 distances of 1.77 and 1.68 Å, respectively. The calculated correlation time at 213 K for H1 and H8 were 4.6×10^{-10} and 3.4×10^{-10} s, respectively.[23] This difference in correlation time values indicates a minor deviation from isotropic molecular motion. However, the effect of anisotropy on the distance results is not severe if distances are calculated from T_1(min) according to Bakhmutov and Berke et al.[50] This is also observed when comparing the results from the T_1(min) approach to the values obtained from the full T_1 curve treatment; i.e., both methods retain similar distance values.

Obviously, both our T_1(min) and full T_1 curve-fitting approaches rely on several assumptions, i.e., interatom distances retrieved from the neutron diffraction study.[51] Therefore, an additional study was performed to confirm the above findings. According to Bakhmutov, a convenient way to study internuclear distances in hydrides is based on measurement of the NOE

buildup rate, i.e., cross-relaxation rate by selective 1D NOE experiments.[52] Selective 1D NOE measurements at 500 MHz were performed to determine the H1···H8 distance at room temperature. Two series of 1D NOE measurements with increasing NOE mixing times were performed; an experiment with selective pulse was applied to the H1 resonance and another one with selective pulse was applied to the methyl resonance at 1.12 ppm. In the first series, the NOE signal buildup at the H8 frequency was monitored, whereas in the second one the NOE buildup of the methyl signal at 1.51 ppm was monitored. The latter experiment served as a reference, where the NOE buildup rate corresponds to an average distance of 3.16 Å between the protons of the two methyl−methyl groups resonating at 1.12 and 1.51 ppm, respectively. The reference distance was computed using the "r^{-3} average" approach utilizing the methyl proton coordinates from the neutron diffraction data.[23,53]

In order to obtain comparable NOE buildup rates, NOE intensities (integrals) were scaled according to $n_A n_B$, where n_A and n_B are the number of chemically equivalent protons in the groups contributing to the NOE signal (scaling factors 1 and 36 for H1−H8 and methyl−methyl, respectively).[53,54] In addition, NOE intensities were corrected for different degree of selective inversion and relaxation effects during excitation sculpting element in the 1D DPFGSE NOE pulse sequence.[55] This was achieved by comparing the integrals of the inverted resonances in the spectra recorded with the shortest mixing time of 12 ms, i.e., to return the integral ratio H1:Me(1.12 ppm) back to 1:6. A correction factor of 0.99 has to be applied to the data obtained from H1 selective 1D NOE.[56] Assuming isotropic molecular motion, the distance between protons H1 and H8 (r_{H1-H8}) can then be calculated using eq 5, where r_{Me-Me} is the reference distance 3.16 Å, while σ_{H1-H8} and σ_{Me-Me} are the cross-relaxation rates (NOE buildup rates) determined from the linear parts of the buildup curves. This results in a value of 1.63 Å for r_{H1-H8}.[23,52] Additional measurements at room temperature using 2D NOESY data resulted in r_{H1-H8} of 1.65 Å.[23]

$$r_{H1-H8} = r_{Me-Me}\sqrt[6]{\frac{\sigma_{Me-Me}}{\sigma_{H1-H8}}} \quad (5)$$

The H1···H8 interproton distances extracted from NMR experiments agree reasonably well with each other and give strong evidence that a structure similar to the one in the solid state determined by neutron and X-ray scattering is maintained in a CD_2Cl_2 solution. Conclusively, the collected NMR data suggests a short dihydrogen bond length range of approximately 1.6−1.8 Å within **NHHB** in solution which is consistent with 1.67 Å determined in the solid state. At temperatures above room temperature the dihydrogen bond distance of **NHHB** in solution is thought to become even shorter, as evidenced above.

FT-IR Spectra. Vibrational spectroscopy is a sensitive probe of the potential energy surface of a molecule which determines the dynamics of its nuclear motion. Based on the Born−Oppenheimer approximation, conclusions can then be drawn on structural and dynamic properties of the matter.[36] We measured FT-IR spectra in the solid state and in solution to further study the dihydrogen bonding in **NHHB** and its deuterated analogues. Due to the large number of atoms in one molecule, the resulting IR spectra are complex.[57] Therefore, we focused on the regions of the N−X and B−Y stretching modes between 1500 and 3200 cm^{-1}. By comparison of the solid-state spectrum of **NHHB** with the spectra of its deuterated analogues (Figure 4) the bands representing the

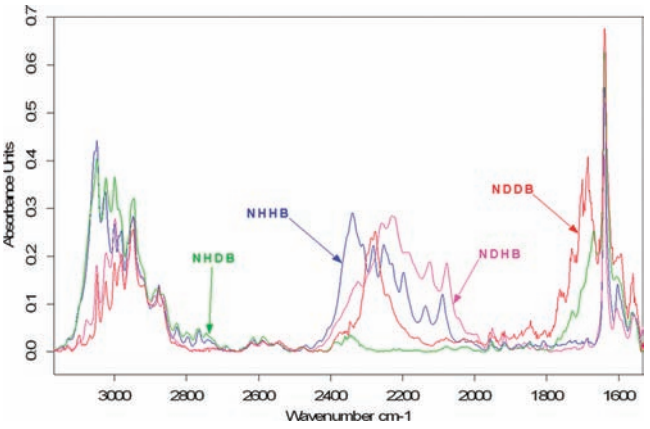

Figure 4. Comparison of solid-state DRAFT spectra of all four isotopic isomers of **NXYB** in the N−X and B−Y stretching frequency region.

Table 3. Frequency Regions of the N−X and B−Y Stretching Modes in the Solid State of NXYB (in cm^{-1})

mode	NHHB	NDDB	NHDB	NDHB
ν(NH)	3110−2970[a]	–	3110−2970[a]	–
ν(ND)	–	2400−2160	–	2440−1980[b]
ν(BH)	2440−2060	–	–	2440−1980[b]
ν(BD)	–	1780−1560	1780−1560	–

[a] The precise region cannot be determined because of overlapping C−H stretching vibrations. [b] Due to a signal overlap it cannot be distinguished between the N−D and B−D stretching modes.

N−X and B−Y stretching modes can be easily identified (Table 3): Due to the isotopic substitution of H by D the corresponding bands shift to lower frequencies.[36] When looking at the data it is obvious that ν(NH) is considerably red-shifted when compared to a non-perturbed NH group above 3500 cm^{-1}. This, and the broadening of the vibration are proofs for the existence of hydrogen bonding—in this case of dihydrogen bonding in the solid which further supports the findings of the neutron diffraction study.[58,59] The shape of the band cannot be discussed in detail because of the overlapping C−H stretching vibrations.

The unusual broadness of the B−H stretching mode and the many maxima can be ascribed to anharmonicity leading to strong coupling between different vibrations—one of them being presumably the N−H stretching mode. This is supported by the different shapes and intensities of the B−D stretching vibrations of **NDDB** and **NHDB** where the influence of the isotopic substitution of the protonic hydron is apparent. The specific shape of the B−H stretching vibration is therefore another direct proof for intramolecular dihydrogen bonding at room temperature as observed in the solid-state structure of **NHHB** determined by neutron diffraction at 10 K. Fermi coupling is also thought to influence the band shape because of the complex pattern of vibrations in the region below 1500 cm^{-1} resulting in a large amount of overtones and combination levels.[36,57]

Upon deuteration the value for ν(NH)/ν(ND) and ν(BH)/ν(BD) should be close to $\sqrt{2}$ in the case of a harmonic oscillator and the line width should also decrease by the inverse of this factor $1/\sqrt{2}$.[60] Because of signal overlap and the broadness of the signals of **NXYB** these values cannot be determined accurately, but the ratio of the frequency shifts are in the region of 1.32−1.34, being

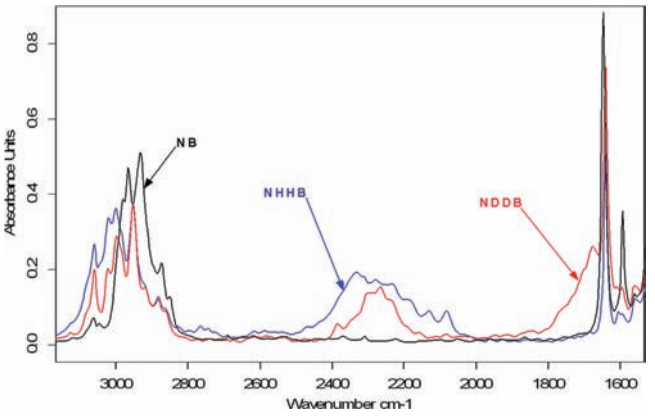

Figure 5. Comparison of solution spectra of **NB**, **NHHB** and **NDDB** in CH_2Cl_2 at 300 K in the N−X and B−Y stretching frequency region. The spectrum of the solvent has been subtracted in all cases.

quite close to the value mentioned above. In earlier publications it was shown that this factor decreases with increasing strength of hydrogen bonds and can even reach unity in the case of strong H-bonds.[36,58] This is not in line with our findings because **NXYB** does exhibit a comparatively strong dihydrogen bond as shown above. On the other hand several differences between the studied systems are obvious. In contrast to **NXYB** the previously studied systems were mainly intermolecular ones. Anomalies have been reported before for intramolecular H-bonding, due to different electronic configurations especially in rings.[58] In addition, no systematic work in this field with regard to dihydrogen bonding is known. High-level quantum mechanical calculations to determine the potential energy surface would be needed for further interpretations of the observed isotope effects.

In the case of solution spectra of **NHHB**, **NDDB**, and **NB** (Figure 5), the N−X and B−Y stretching vibrations can again be identified easily, and do not differ apparently in their location (see Table 3 for solid-state values). This finding coincides with the result of the ^{1}H NMR T_1 relaxation study because it is a clear proof for strong intramolecular dihydrogen bonding in solution. The biggest difference seems to be in the N−H stretching mode, but since the spectrum of the solvent had to be subtracted in this region no detailed interpretation is possible. The equilibria between different structural isomers, as pointed out before, could not be studied at variable temperatures because no significant differences were detected in the spectra of solutions between 240 and 380 K.[57] The changes that occur are presumably obscured by the broadness of the bands. This is remarkable because above 338 K **NHHB** is destabilized and releases dihydrogen slowly. Therefore it is assumed that the structure of the molecule—in particular the dihydrogen bond and its intramolecular nature—is quite stable in solution until the loss of H_2 occurs and **NB** is formed with the only change being the N−H and H−H distances as mentioned above.

In addition, VT solution spectra of **NHHB**, **NDDB**, and **NB** (only 300 K) were recorded in the low wavenumber region (600−100 cm^{-1}) where the stretching vibration of the dihydrogen bond was assumed to be located.[57] A rather large number of bands was observed and a distinct assignment could not be made. A normal coordinate analysis is mandatory for further investigations in this respect.[61] An increase or decrease in intensity could also not be observed upon temperature variations as reported previously for dihydrogen bonds in other systems.[62]

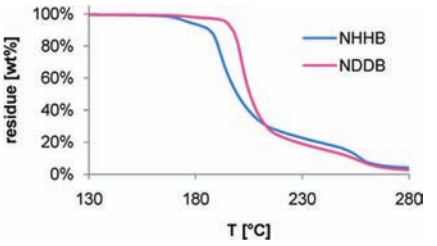

Figure 6. TG curves of **NHHB** and **NDDB** at heating rates of 5 °C/min.

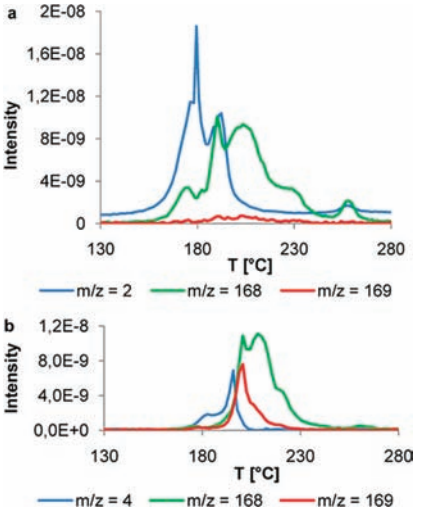

Figure 7. Selected MS signals of TG-MS measurements of (a) **NHHB** and (b) **NDDB** at a heating rate of 5 °C/min.

TG-MS Measurements. The solid ionic pairs ammonium borohydride and diammoniate of diborane which also consist of N−H···H−B dihydrogen bonds are known to release hydrogen gas upon heating in the solid state starting at temperatures above −40 and 85 °C, respectively.[62] Since **NXYB** can release XY in solution forming **NB** the question was raised whether this is also possible in the solid state. Therefore thermogravimetry (TG) measurements of the pure solids **NHHB** and **NDDB** were conducted under a flow of nitrogen at heating rates of 5 °C/min. As can be seen in Figure 6, **NHHB** starts to decompose at 165 °C, and at 185 °C already 7.5 wt % is lost. Because **NHHB** contains only 0.34 wt % of stored hydrogen, this significant mass loss results out of a degradation of the **NB** backbone. **NDDB** on the other hand follows reproducibly different kinetics: decomposition starts at slightly higher temperatures around 170 °C and proceeds very slowly. At 185 °C only 1.5 wt % of the initial mass is lost. At the same time it has to be considered that 0.69 wt % of **NDDB** corresponds to the stored D_2. Therefore, besides D_2 release, also partial decomposition of the **NB** structure starts. At the same time the calculated transition temperatures, taken as $\Delta G = 0$ kJ/mol for the hydrogen-releasing reaction using the data of Table 1, are at 170 and 200 °C for **NHHB** and **NDDB**, respectively.

To gain insight into the initial decomposition products upon heating, scans of different masses were recorded on a coupled EI-MS. The intensities of the largest m/z signals are depicted in Figure 7. The signal with a value of 2 amu in Figure 7a can be

assigned to H_2^+ and 168 amu most probably to $C_6HF_5^+$. It can clearly be seen that both fragments are detected simultaneously in the beginning with increasing intensities. To analyze whether the H_2^+ ion is the stored hydrogen or results from another part of the molecule the same measurements were conducted on **NDDB**. Figure 7b shows that D_2^+ (m/z = 4 amu) is indeed detected at temperatures around 170 °C together with $C_6HF_5^+$ (m/z = 168 amu) and $C_6DF_5^+$ (m/z = 169 amu). The first and the latter signals are both missing in the TG-MS experiment with **NHHB**. This—together with the observation that **NDDB** is thermodynamically more stable than **NHHB**—leads to the following conclusions: (1) The structure **NXYB** is stabilized by XY. (2) Once XY is released the residue decomposes quite fast. (3) The perfluorinated phenyl rings are among the first parts of **NXYB** that break up. (4) **NDDB** seems to experience a greater stabilization by the stronger N−D···D−B bond in comparison to the N−H···H−B bond in **NHHB**. The data in Table 1 support the smaller ZPE of **NDDB** compared to **NHHB** as a reason for this stabilization. At the same time this difference is larger than in D_2/H_2.[23] About half of this isotopic effect arises from the N−D and B−D stretching modes, and the remaining part has its origin in the coupled modes between N−D, B−D and other functional groups.[23]

Additionally a signal corresponding to HD^+ (m/z = 3 amu) could also be detected simultaneously to D_2^+ during heat-up of **NDDB**.[23] This also points to an uncontrolled degradation of **NXYB** rather than a clean XY release. In summary, it was not possible to release H_2 or D_2 in the solid state leaving the intact compound **NB** behind. A similar behavior could be observed upon heating of **NHHB** under vacuum at 150 °C. It seems that especially the B−C_6F_5 bondings are thermally too instable to allow such an H_2 release from the solid state. At isothermal conditions the release of H_2 (145 °C) or D_2 (165 °C) was also always accompanied by decomposition products of the **NB** backbone.

CONCLUSIONS

Besides the previously reported **NHHB**, we could successfully synthesize the individual, deuterated isomers **NDDB**, **NHDB**, and **NDHB**. They were characterized by HRESI-TOF mass spectrometry, multinuclear NMR, and IR spectroscopy.

We have determined the crystal structure of **NHHB** by neutron diffraction and could show that an extremely short intramolecular dihydrogen bond exists with an H···H contact of only 1.67 Å. TG-MS studies of **NXYB** showed that XY cannot be released in the solid state without immediate degradation of **NB**. The decomposition of **NHHB** begins at 145 °C and around 165 °C in the case of **NDDB**. The N−X and B−Y stretching vibrations were identified in FT-IR spectra of the solids. A red shift of ν(NX), the broadness of the ν(NX) and ν(BY) bands, and the fact that several maxima are present in the latter case are explained by Fermi couplings and anharmonicity. This supports the existence of dynamic intramolecular dihydrogen bonding in the solid state at room temperature. The ratios of ν(NH)/ν(ND) and ν(BH)/ν(BD) are in the region of 1.32−1.34.

By dilution, VT and 2D NOESY NMR spectroscopic experiments the dynamic nature of **NHHB** in solution was studied, and the part of the molecule in close proximity to the N atom was identified to be in constant change. An equilibrium between at least two conformational isomers (**NHHB(1/2)**) exists, with one more stable and hence preferred isomer. Upon deuterium labeling of **NHHB** a primary isotope effect could be identified by ^{1}H NMR spectroscopy: the chemical shift difference $^P\Delta^1$H-(D) = δ(N*H*) − δ(N*D*) amounts to 0.56 ppm. It could be shown that this chemical shift difference is caused by different positions of D and H in the hydrogen bond. ^{1}H NMR spectroscopic T_1 relaxation and selective 1D NOE measurements showed that the N−H···H−B dihydrogen bond length is 1.6−1.8 Å—very close to the value determined in the solid by neutron diffraction—and even shorter at elevated temperatures. FT-IR spectra of **NHHB**, **NDDB**, and **NB** support this finding because of very similar frequencies and band shapes of the N−X and B−Y stretching vibrations in solid and solution spectra. In addition, no structural changes could be detected in VT FT-IR studies (240−380 K) upon cooling and heating of the solutions. Furthermore, only the N-bound hydron in **NXYB** can easily be exchanged in solution, and even upon heating no rotation of X···Y occurs until XY is released.

Upon the activation of deuterium hydride by **NB**, no isotope effect with regard to H/D distribution was detected.[38] Theoretical calculations attribute this to an early transition state. The valuable insights into structures, reactivity, and mechanisms revealed in this article will be useful for further developments of FLP based hydrogenation catalysts.

EXPERIMENTAL SECTION

General Methods and Materials. Whenever necessary, the experiments were performed on double-manifold H_2 (D_2, HD, Ar)/vacuum lines or in an argon glovebox (MBraun Labmaster 130). Dichloromethane, *n*-pentane, and toluene were dried by an MBraun solvent purification system (MB SPS-800). Deuterated solvents were received from Deutero GmbH, dried by stirring over CaH_2 overnight at room temperature, and distilled prior to use. Hydrogen gas (5.0) was purchased from Linde and passed through a drying unit equipped with molecular sieves (4 Å). D_2 (99.96%) and HD (98%) lecture bottles were obtained from Isotec and used without further purification. Methanol (extra dry) and benzene (anhydrous) were purchased from Acros Organics and Sigma-Aldrich and used as received. 1,1,2,2-Tetrachloroethane (Acros Organics) was dried by stirring over CaH_2 overnight at room temperature and distilled prior to use. 1-*N*-TMP-CH_2-2-[B(C_6F_5)$_2$]C_6H_4 (**NB**)[11] and 1-*N*-TMPH-CH_2-2-[HB(C_6F_5)$_2$]C_6H_4 (**NHHB**)[11] were synthesized as described previously.

NMR and VT-NMR experiments were performed on a Bruker ARX-300 spectrometer (^{1}H, ^{11}B, ^{19}F) or a Bruker DPX-400 (^{2}H). ^{1}H (^{2}H) NMR spectra are referenced to $SiMe_4$ ($SiMe_4$-d_{12}) by referencing the residual solvent peak (also during low-temperature studies). ^{11}B and ^{19}F NMR spectra were referenced externally to $BF_3\cdot Et_2O$ at 0 ppm and CF_3CO_2H at −78.5 ppm relative to $CFCl_3$ at 0 ppm, respectively.

All 2D ^{1}H,^{1}H NOESY NMR measurements were performed at 27 °C using a Varian Unity Inova 500 spectrometer (500 MHz ^{1}H-frequency) equipped with a 5 mm ^{1}H-{X} pulsed field gradient inverse detection probe head. The standard sample preparation inside an argon glovebox was to weigh 15 mg in total of pure or mixtures of crystalline **NXYB** in 5 mm NMR tubes and dissolve it in 0.5 mL of carefully dried CD_2Cl_2 or C_6D_6. One-dimensional ^{1}H NMR spectra from each sample were recorded prior to NOESY measurements. Spectra covering a spectral width of 5497.5 Hz were recorded using a 90° pulse with 64 transients preceded by two steady-state scans. The relaxation delay was 10.0 s and the number of acquired complex data points was 10 382 (acquisition time 1.9 s). The FID was multiplied by an exponential weighting function with a 5 Hz line-broadening factor and zero-filled up to 16 384 complex data points prior to Fourier transformation. Polynomial baseline correction was applied (fifth order) and the receiver gain was kept constant in every measurement. The pulse width was determined for

each sample and variation in pulse lengths was below 5%, confirming nonsignificant differences in dielectric loading of RF-coil and thus in the sensitivity. Signal integrals were determined using the spectrometer operating software VNMR 6.1C. To determine scaling factors in order to normalize integration results in 1D as well as in NOESY with respect to small differences in sample concentrations, signals of methylene protons (4.5 ppm in CD_2Cl_2, 4.8 ppm in C_6D_6) were integrated. Note that in C_6D_6 solution, methylene protons overlap with approximately half of the boron-bound signals. In C_6D_6, the B*H* signal integral is evaluated by integrating half of the signal (overlap-free) to avoid the CH_2 signal and the final result was multiplied by 2. Half of the B*H* integral is also subtracted from the CH_2 integral data to correct for the effect of overlap before correction factor calculation. In the CD_2Cl_2 samples, part of the N*H* signal (at 7.9 ppm) overlaps with aromatic proton signals. Therefore, only the low-field half of the signal (from 7.9 to 8.6 ppm) is integrated and the result is multiplied by 2.

Two-dimensional NOESY spectra were recorded to estimate the portion of **NHHB** in the samples by comparison of cross-peak volumes between N*H* and B*H* protons. NOESY spectra were recorded in phase sensitive mode using a spectral width of 5497.53 Hz in both dimensions. Spectra were recorded using 32 transients and 200 increments. The number of acquired complex data points was 1100. NOESY mixing time was 600 ms and a relaxation delay of 2.0 s was used. Receiver gain was kept constant in all NOESY measurements. Time domain data was apodized using Gaussian function and zero-filled to 2048 complex points in both dimensions, prior to Fourier transformation. Polynomial baseline correction (fifth order) was applied in f_2-dimension before 2D integration. Integration of the NOESY correlation peak between N*H* and B*H* protons was accomplished using the VNMR 6.1C software. Due to partial overlap of N*H*−*H*B correlation with N*H*−H_2C and $H_{(aromatic)}$−H_2C correlations, only approximately half of the N*H*−*H*B cross-peak (nonoverlapping part) was included in the integration area. To obtain the estimate of total cross-peak volume, the integration result was multiplied by 2. Before comparison of N*H*−*H*B cross-peak volumes, the volume data was normalized using correction factors calculated from 1D data (see above).

NOESY spectra were recorded from the following samples: **NHHB** in CD_2Cl_2, equimolar amounts of **NHDB** and **NDHB** in CD_2Cl_2, **NHHB** in C_6D_6, equimolar amounts of **NHDB** and **NDHB** in C_6D_6, **NB** that reacted with HD dissolved in CD_2Cl_2, **NB** that reacted with HD dissolved in C_6D_6.

^{1}H T_1 relaxation measurements were carried out by the standard inversion−recovery (180°−τ−90°) method with the use of a Bruker ARX-300 spectrometer in deoxygenated CD_2Cl_2 solutions. Calculations of the relaxation times were completed using the nonlinear three-parameter fitting routine of the spectrometer. In order to determine the minimum T_1 times (T_1(min)), the experiments were performed in the temperature range of 183−293 K. Fitting of the T_1 curves to the T_1 values measured at different temperatures was accomplished via the MS Excel Solver routine utilizing the GRG2 quasi-Newton nonlinear regression algorithm.[63] The T_1(min) values of all protons were determined at 213 K.

Selective 1D NOE measurements were conducted with a Varian Unity Inova 500 spectrometer at 27 °C equipped with a 5 mm ^{1}H-{X} pulsed field gradient inverse detection probe head using the 1D double-pulsed field-gradient-spin-echo nuclear Overhauser effect (DPFGSE-NOE) pulse sequence.[55] Selective inversion of H1 resonances was accomplished using a 5.4 ms 180° Gaussian pulse applied at an RF-power of 210 Hz, whereas a 15.5 ms 180° Gaussian pulse at an RF-power of 74 Hz was used for the methyl resonance at 1.12 ppm. Hard rectangular pulses were applied at an RF-power of 37 kHz. Selective experiments for H8 were not successful, since rapid transverse relaxation of H8 during selective pulses as well as pulsed field gradient periods led to complete disappearance of the signal. NOE mixing times were 12, 20, 30, 40, 60, 100, 120, 150, and 200 ms. Spectra were recorded with 64 transients, keeping receiver gain constant in every measurement. The spectral width was 5497.5 Hz, the relaxation delay was 5.0 s, and the number of acquired complex data points was 10 995 (acquisition time 2.0 s). The FID was multiplied by an exponential weighting function with a line-broadening factor of 3 Hz and zero-filled up to 16 384 complex data points prior to Fourier transformation. A baseline correction using a spline function was applied prior to the integration of NOE peaks.

VT FT-IR studies (4000−100 cm^{-1}) of dissolved samples (concentrations: 0.01−0.5 mol/L) were conducted on a Bruker VERTEX 70 with a VT cell from Specac including a temperature controller. For the low-temperature measurements liquid nitrogen was used for cooling. The samples were dissolved inside an argon glovebox (MBraun Labmaster 130) where the resulting solutions were transferred into the cell in order to exclude any traces of water. The measurements in the low frequency range (300−600 cm^{-1}) were performed with polyethylene as window material (d = 1 mm). Unfortunately, it was impossible to provide the measurements in the range below 300 cm^{-1} at temperatures below room temperature due to the strong bands of the media CH_2Cl_2. The use of other solvents was restricted because of the poor solubility of the zwitterions in low polar solvents (toluene and linear hydrocarbons). At room temperature and above C_6H_6 was used and hence spectra ranging from 100 to 600 cm^{-1} were obtained. The measurements in the medium frequency range (800−4000 cm^{-1}) were performed using AgCl windows (d = 100 μm). Unfortunately, it was impossible to provide the measurements in the range below 800 cm^{-1} at room temperature and lower due to the strong bands of the media CH_2Cl_2. Above room temperature 1,1,2,2-tetrachloroethane was used and hence spectra ranging from 850 to 4000 cm^{-1} were obtained. Diffuse reflection−absorption FT-IR spectra (DRAFT) without solvent were recorded on a Bruker VERTEX 70 by deposition of small amounts of pulverized substance on the reflecting metal plate of a DRIFT unit (Spectra Tech: The Collector).[64]

High-resolution mass spectra (HRESI-TOF) were recorded on a Bruker micrOTOF-Q mass spectrometer utilizing acetonitrile as solvent.

TG-MS experiments were carried out on a Q5000 thermogravimetric analyzer from TA Instruments connected to an HPR-20 from Hiden Analytical.

Crystals suitable for neutron diffraction were grown from a benzene-d_6 solution. **NHHB** was dissolved in C_6D_6 at 60 °C in a Schlenk tube under an argon atmosphere to obtain a saturated solution. After addition of a seed crystal, it was slowly cooled to 35 °C where a large crystal formed after several days. The temperature was finally lowered to room temperature and a single crystal of the size 2 × 2 × 2 mm could be obtained. The neutron diffraction study of **NHHB** was carried out on thermal single crystal diffractometer RESI[65] at FRM II, equipped with a Huber Eulerian cradle and a SHI RDK-101 cryostat at 10.0(1) K using the Cu-422 monochromator (λ = 1.03(1) Å). The X-ray structure was used as a starting point for full-matrix least-squares refinement on F (JANA2000/JANA2006[66]). The H atoms were refined free, and the disordered solvent molecules were treated as rigid bodies with ideal geometry. All atoms were refined with isotropic thermal displacement parameters. Extinction was treated in an isotropic Becker-Coppens model as implemented in JANA2006.[67] Some bond distances are presented in Table 4, and the structure is shown in Figure 8.

NHHB. Colorless crystal, $C_{28}H_{26}BF_{10}N \cdot 0.5C_6D_6$, M = 619.38 g/mol, crystal size 2 × 2 × 2 mm, T = 10 K, triclinic, space group $P\bar{1}$ (No.2), a = 10.587(10) Å, b = 12.183(10) Å, c = 12.520(10) Å, α = 86.77(5)°, β = 70.73(5)°, γ = 64.83(5)°, V = 1372.95(2) Å^3, Z = 2, ρ(calcd) = 1.498 Mg/m^3, F(000) = 400, μ = 0.071 mm^{-1}, 9015 reflexes ($2\theta_{max}$ = 110°), 5332 > 2.5σ [R_{int} = 7.0%], 295 parameters, $R1$ ($I > 2.5\sigma(I)$) = 0.066, w$R2$ (*all data*) = 0.065, GooF = 1.42, largest diff. peak and hole 1.56 and −1.40 barns/Å^3.

Table 4. Selected Bond Distances As Determined by Neutron Diffraction

bond	distance [Å]
d(B1−H1)	1.235(7)
d(N8−H8)	1.033(6)
d(H1−H8)	1.674(8)

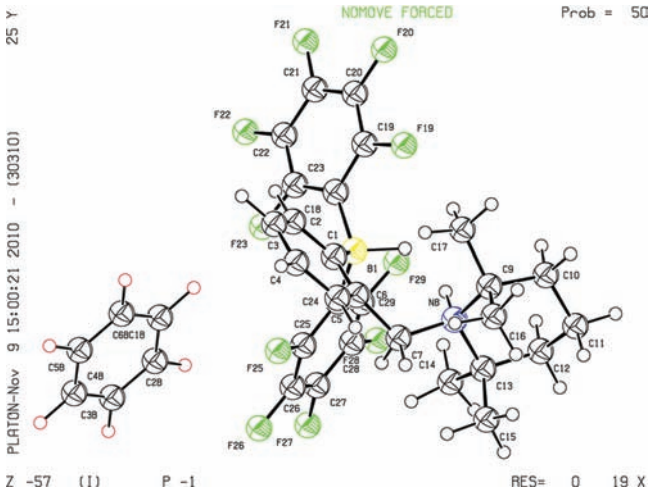

Figure 8. ORTEP plot of the crystal structure of **NHHB** as determined by neutron diffraction. Black circles, H; red circles, D.

NMR Measurements of 1-*N*-TMPH-CH_2-2-[$HB(C_6F_5)_2$]C_6H_4 (NHHB). ^{1}H NMR (CD_2Cl_2, 300 MHz): δ 7.77 (br s, 1H, N*H*), δ 7.16 (m, 4H, C_6H_4), δ 4.45 (d, 2H, $^3J_{HH}$ = 5.5 Hz, NCH_2), δ 3.76 (br q, 1H, $^1J_{HB}$ = 77 Hz, B*H*), δ 1.6−1.9 (m, 6H, $CH_2CH_2CH_2$), δ 1.51 (s, 6H, CH_3), δ 1.13 (s, 6H, CH_3). ^{11}B NMR (CD_2Cl_2, 96 MHz): δ −20.84 (d, $^1J_{BH}$ = 78 Hz). ^{19}F NMR (CD_2Cl_2, 282 MHz): δ −133.44 (d, 6F, $^3J_{FF}$ = 22 Hz, *o*-C_6F_5), δ −163.45 (br s, 3F, *p*-C_6F_5), δ −166.85 (m, 6F, *m*-C_6F_5).

Synthesis of 1-*N*-TMPD-CH_2-2-[$DB(C_6F_5)_2$]C_6H_4 (NDDB). In a glovebox, a 25-mL flame-dried Schlenk tube equipped with a stir bar, a Teflon stopcock and a glass stopper (Glindemann sealing rings were used for conical joints instead of grease) was charged with 1-*N*-TMP-CH_2-2-[$B(C_6F_5)_2$]C_6H_4 (**NB**, 1.0 mmol, 575 mg), and 3 mL of dry *n*-pentane. The reaction was degassed once with a freeze−pump−thaw cycle and refilled with D_2 (1 bar). The reaction was stirred at 1000 rpm at room temperature for 15 min and a white precipitate formed. After filtration and washing (five times) with *n*-pentane (15 mL), 568 mg (1.0 mmol, 98%) of **NDDB** was obtained as a white solid. ^{1}H NMR (CD_2Cl_2, 300 MHz): δ 7.15 (m, 4H, C_6H_4), δ 4.44 (s, 2H, NCH_2), δ 1.6−1.9 (m, 6H, $CH_2CH_2CH_2$), δ 1.51 (s, 6H, CH_3), δ 1.12 (s, 6H, CH_3). ^{2}H NMR (CH_2Cl_2, 400 MHz): δ 7.21 (br s, 1D, N*D*), δ 3.76 (br s, 1D, B*D*). ^{11}B NMR (CD_2Cl_2, 96 MHz): δ −21.07 (s). ^{19}F NMR (CD_2Cl_2, 282 MHz): δ −133.67 (d, 6F, $^3J_{FF}$ = 22 Hz, *o*-C_6F_5), δ −163.66 (br s, 3F, *p*-C_6F_5), δ −167.03 (m, 6F, *m*-C_6F_5). HRMS ESI$^+$-TOF calcd for $C_{28}H_{25}BDF_{10}N\cdot Na^+$: 601.1954. Found: 601.1931. HRMS ESI$^-$-TOF calcd for $C_{28}H_{24}BDF_{10}N^-$: 577.1989. Found: 577.1992.

Synthesis of 1-*N*-TMPD-CH_2-2-[$HB(C_6F_5)_2$]C_6H_4 (NDHB). In a glovebox, a 25-mL flame-dried Schlenk tube equipped with a stir bar, a Teflon stopcock, and a glass stopper (Glindemann sealing rings were used for conical joints instead of grease) was charged with 1-*N*-TMPH-CH_2-2-[$HB(C_6F_5)_2$]C_6H_4 (**NHHB**, 0.35 mmol, 200 mg) and 3 mL of a methanol-d_1/benzene (40/60) mixture. The reaction was stirred at 1000 rpm at room temperature overnight. After evaporation of the solvents in vacuo, this procedure was repeated once more. Subsequent washing (three times) with *n*-pentane (6 mL) yielded 188 mg (0.33 mmol, 94%) of **NDHB** as a white solid. ^{1}H NMR (CD_2Cl_2, 300 MHz): δ 7.15 (m, 4H, C_6H_4), δ 4.44 (s, 2H, NCH_2), δ 3.72 (br q, 1H, $^1J_{HB}$ = 76 Hz, B*H*), δ 1.6−1.9 (m, 6H, $CH_2CH_2CH_2$), δ 1.51 (s, 6H, CH_3), δ 1.12 (s, 6H, CH_3). ^{2}H NMR (CH_2Cl_2, 400 MHz): δ 7.20 (br s). ^{11}B NMR (CD_2Cl_2, 96 MHz): δ −20.86 (d, $^1J_{BH}$ = 77 Hz). ^{19}F NMR (CD_2Cl_2, 282 MHz): δ −133.67 (d, 6F, $^3J_{FF}$ = 22 Hz, *o*-C_6F_5), δ −163.66 (br s, 3F, *p*-C_6F_5), δ −167.06 (m, 6F, *m*-C_6F_5). HRMS ESI$^+$-TOF calcd for $C_{28}H_{26}BF_{10}N\cdot Na^+$: 600.1891. Found: 600.1903. HRMS ESI$^-$-TOF calcd for $C_{28}H_{25}BF_{10}N^-$: 576.1926. Found: 576.1930.

Synthesis of 1-*N*-TMPH-CH_2-2-[$DB(C_6F_5)_2$]C_6H_4 (NHDB). In a glovebox, a 25-mL flame-dried Schlenk tube equipped with a stir bar, a Teflon stopcock, and a glass stopper (Glindemann sealing rings were used for conical joints instead of grease) was charged with 1-*N*-TMPD-CH_2-2-[$DB(C_6F_5)_2$]C_6H_4 (**NDDB**, 0.35 mmol, 200 mg) and 3 mL of a methanol/benzene (40/60) mixture. The reaction was stirred at 1000 rpm at room temperature overnight. After evaporation of the solvents in vacuo, this procedure was repeated once more. Subsequent washing (three times) with *n*-pentane (6 mL) yielded 191 mg (0.33 mmol, 95%) of **NHDB** as a white solid. ^{1}H NMR (CD_2Cl_2, 300 MHz): δ 7.70 (br s, 1H, N*H*), δ 7.16 (m, 4H, C_6H_4), δ 4.44 (d, 2H, $^3J_{HH}$ = 5.5 Hz, NCH_2), δ 1.6−1.9 (m, 6H, $CH_2CH_2CH_2$), δ 1.51 (s, 6H, CH_3), δ 1.12 (s, 6H, CH_3). ^{2}H NMR (CH_2Cl_2, 400 MHz): δ 3.80 (br s). ^{11}B NMR (CD_2Cl_2, 96 MHz): δ −21.15 (s). ^{19}F NMR (CD_2Cl_2, 282 MHz): δ −133.66 (d, 6F, $^3J_{FF}$ = 22 Hz, *o*-C_6F_5), δ −163.63 (br s, 3F, *p*-C_6F_5), δ −167.02 (m, 6F, *m*-C_6F_5). HRMS ESI$^+$-TOF calcd for $C_{28}H_{25}BDF_{10}N\cdot Na^+$: 601.1954. Found: 601.2017. HRMS ESI$^-$-TOF calcd for $C_{28}H_{24}BDF_{10}N^-$: 577.1989. Found: 577.2015.

Reaction of 1-*N*-TMP-CH_2-2-[$B(C_6F_5)_2$]C_6H_4 (NB) with Deuterium Hydride. In a glovebox, a 25-mL flame-dried Schlenk tube equipped with a stir bar, a Teflon stopcock, and a glass stopper (Glindemann sealing rings were used for conical joints instead of grease) was charged with 1-*N*-TMP-CH_2-2-[$B(C_6F_5)_2$]C_6H_4 (**NB**, 0.4 mmol, 230 mg) and 1.5 mL of dry *n*-pentane. The reaction was degassed once with a freeze−pump−thaw cycle and refilled with D_2 (1 bar). The reaction was stirred at 1000 rpm at room temperature for 15 min and a white precipitate formed. After filtration and washing (five times) with *n*-pentane (5 mL), 227 mg (0.4 mmol, 98%) of a white solid was obtained. ^{1}H NMR (CD_2Cl_2, 300 MHz): δ 7.76 (br s, 0.5H, N*H*), δ 7.14 (m, 4H, C_6H_4), δ 4.44 (overlap of s and d, 2H, NCH_2), δ 3.72 (br q, 1H, $^1J_{BH}$ = 76 Hz, B*H*), δ 1.6−1.9 (m, 6H, $CH_2CH_2CH_2$), δ 1.51 (s, 6H, CH_3), δ 1.12 (s, 6H, CH_3). ^{2}H NMR (CH_2Cl_2, 400 MHz): δ 7.23 (br s, 1D, N*D*), δ 3.78 (br s, 1D, B*D*). ^{11}B NMR (CD_2Cl_2, 96 MHz): δ −20.81 (overlap of s and d). ^{19}F NMR (CD_2Cl_2, 282 MHz): δ −133.67 (d, 6F, $^3J_{FF}$ = 22 Hz, *o*-C_6F_5), δ −163.66 (br s, 3F, *p*-C_6F_5), δ −167.05 (m, 6F, *m*-C_6F_5). HRMS ESI$^+$-TOF calcd for $C_{28}H_{25}BDF_{10}N\cdot Na^+$: 601.1954. Found: 601.1929. HRMS ESI$^+$-TOF calcd for $C_{28}H_{26}BF_{10}N\cdot Na^+$: 600.1891. Found: 600.1911. HRMS ESI$^-$-TOF calcd for $C_{28}H_{24}BDF_{10}N^-$: 577.1989. Found: 577.1994. HRMS ESI$^-$-TOF calcd for $C_{28}H_{25}BF_{10}N^-$: 576.1926. Found: 576.1977.

Theoretical Analysis. The calculations were carried out using DFT with the PBE[68] and CAM-B3LYP[69] functionals and a 6-31G** basis set[70] for all atoms. The computed structures were presented in our earlier paper.[11] The effects of the hydrogen−deuterium isotopic substitution are new. Gaussian 09[71] was employed for the DFT calculations. In addition, a potential energy distribution analysis was performed by the VEDA program.[72]

■ ASSOCIATED CONTENT

Supporting Information. Characterization of compounds by multinuclear NMR spectroscopy, packing diagrams, and geometric parameters from single-crystal neutron diffraction analysis; crystallographic data and CIF file; FTIR DRAFT and VT-FTIR

solution spectra; ^{1}H NMR T_1 relaxation data, 2D NOESY spectra, VT-NMR spectra and MS signals of TG-MS measurements; complete ref 71. This material is available free of charge via the Internet at http://pubs.acs.org.

AUTHOR INFORMATION

Corresponding Author
timo.repo@helsinki.fi; rieger@tum.de

ACKNOWLEDGMENT

We gratefully acknowledge the beam time obtained at FRM II, the neutron source at the Technische Universität München. We thank G. Gemmecker, K. Ruhland, S. Vagin, K. Chernichenko, J. Dengler, A. Jonovic, and P. Heinz for help with the data collections and S. Vagin for helpful discussions. The work was funded by the Academy of Finland (123248, 139550) and DAAD (D/05/51658). P.P. belongs to the Finnish Centre of Excellence in Computational Molecular Science. M.A. thanks the Swedish Institute.

REFERENCES

(1) Kubas, G. J. *Metal Dihydrogen and σ-Bond Complexes: Structure, Theory and Reactivity*; Kluwer Academic/Plenum Publishers: New York, 2001.

(2) (a) Brunner, H. Hydrogenation. In *Applied Homogeneous Catalysis with Organometallic Compounds*; Cornils, B., Herrmann, W. A., Eds.; VCH: Weinheim, 1996; Vol. 1. (b) Weissermel, K.; Arpe, H.-J. *Industrial Organic Chemistry*, 3rd ed.; VCH: Weinheim, 1997. (c) Chenier, P. J. *Survey of Industrial Chemistry*, 3rd ed.; Kluwer Academic/Plenum Publishers: New York, 2002. (d) Wittcoff, H. A.; Reuben, B. G.; Plotkin, J. S. *Industrial Organic Chemicals*, 2nd ed.; John Wiley & Sons: Hoboken, 2004. (e) Hagen, J. *Industrial Catalysis*, 2nd ed.; Wiley-VCH: Weinheim, 2006. (f) Cooke, S. J. Industrial Gases. In *Handbook of Industrial Chemistry and Biotechnology*, 11th ed.; Kent, J. A., Ed.; Springer: New York, 2007; Vol. 2.

(3) Hartwig, J. F. *Organotransition Metal Chemistry: From Bonding to Catalysis*; University Science Books: Mill Valley, CA, 2010.

(4) See for an overview the following recent review articles, and the references therein: (a) Kubas, G. J. *Chem. Rev.* **2007**, *107*, 4152–4205. (b) De Lacey, A. L.; Fernández, V. M.; Rousset, M.; Cammack, R. *Chem. Rev.* **2007**, *107*, 4304–4330. (c) Kubas, G. J. *J. Organomet. Chem.* **2009**, *694*, 2648–2653.

(5) Kubas, G. J.; Ryan, R. R.; Swanson, B. I.; Vergamini, P. J.; Wasserman, H. J. *J. Am. Chem. Soc.* **1984**, *106*, 451–452.

(6) Richardson, T. B.; de Gala, S.; Crabtree, R. H.; Siegbahn, P. E. M. *J. Am. Chem. Soc.* **1995**, *117*, 12875–12876.

(7) (a) Welch, G. C.; Juan, R. R. S.; Masuda, J. D.; Stephan, D. W. *Science* **2006**, *314*, 1124–1126. (b) Spies, P.; Erker, G.; Kehr, G.; Bergander, K.; Fröhlich, R.; Grimme, S.; Stephan, D. W. *Chem. Commun.* **2007**, 5072–5074. (c) Welch, G. C.; Stephan, D. W. *J. Am. Chem. Soc.* **2007**, *129*, 1880–1881. (d) McCahill, J. S. J.; Welch, G. C.; Stephan, D. W. *Angew. Chem., Int. Ed.* **2007**, *46*, 4968–4971. (e) Kenward, A. L.; Piers, W. E. *Angew. Chem., Int. Ed.* **2008**, *47*, 38–41. (f) Geier, S. J.; Gilbert, T. M.; Stephan, D. W. *J. Am. Chem. Soc.* **2008**, *130*, 12632–12633. (g) Huber, D. P.; Kehr, G.; Bergander, K.; Fröhlich, R.; Erker, G.; Tanino, S.; Ohki, Y.; Tatsumi, K. *Organometallics* **2008**, *27*, 5279–5284. (h) Spies, P.; Kehr, G.; Bergander, K.; Wibbeling, B.; Fröhlich, R.; Erker, G. *Dalton Trans.* **2009**, 1534–1541. (i) Stephan, D. W. *Dalton Trans.* **2009**, 3129–3136. (j) Mömming, C. M.; Otten, E.; Kehr, G.; Fröhlich, R.; Grimme, S.; Stephan, D. W.; Erker, G. *Angew. Chem., Int. Ed.* **2009**, *48*, 6643–6646. (k) Jiang, C.; Blacque, O.; Berke, H. *Organometallics* **2009**, *28*, 5233–5239. (l) Ramos, A.; Lough, A. J.; Stephan, D. W. *Chem. Commun.* **2009**, 1118–1120. (m) Geier, S. J.; Stephan, D. W. *J. Am. Chem. Soc.* **2009**, *131*, 3476–3477. (n) Dureen, M. A.; Welch, G. C.; Gilbert, T. M.; Stephan, D. W. *Inorg. Chem.* **2009**, *48*, 9910–9917. (o) Stephan, D. W.; Erker, G. *Angew. Chem., Int. Ed.* **2010**, *49*, 46–76. (p) Power, P. P. *Nature* **2010**, *463*, 171–177. (q) Webb, J. D.; Laberge, V. S.; Geier, S. J.; Stephan, D. W.; Crudden, C. M. *Chem.—Eur. J.* **2010**, *16*, 4895–4902. (r) Jiang, C. F.; Blacque, O.; Berke, H. *Organometallics* **2010**, *29*, 125–133. (s) Neu, R. C.; Ouyang, E. Y.; Geier, S. J.; Zhao, X. X.; Ramos, A.; Stephan, D. W. *Dalton Trans.* **2010**, *39*, 4285–4294. (t) Alcarazo, M.; Gomez, C.; Holle, S.; Goddard, R. *Angew. Chem., Int. Ed.* **2010**, *49*, 5788–5791. (u) Inés, B.; Holle, S.; Goddard, R.; Alcarazo, M. *Angew. Chem.* **2010**, *122*, 8567–8569. (v) Berkefeld, A.; Piers, W. E.; Parvez, M. *J. Am. Chem. Soc.* **2010**, *132*, 10660–10661. (w) Zhao, X. X.; Stephan, D. W. *Chem. Commun.* **2011**, *47*, 1833–1835.

(8) Rokob, T. A.; Hamza, A.; Pápai, I. *J. Am. Chem. Soc.* **2009**, *131*, 10701–10710.

(9) Chapman, A. M.; Haddow, M. F.; Orton, J. P. H.; Wass, D. F. *Dalton Trans.* **2010**, *39*, 6184–6186.

(10) (a) Ullrich, M.; Lough, A. J.; Stephan, D. W. *J. Am. Chem. Soc.* **2009**, *131*, 52–53. (b) Ullrich, M.; Lough, A. J.; Stephan, D. W. *Organometallics* **2010**, *29*, 3647–3654.

(11) Sumerin, V.; Schulz, F.; Atsumi, M.; Wang, C.; Nieger, M.; Leskelä, M.; Repo, T.; Pyykkö, P.; Rieger, B. *J. Am. Chem. Soc.* **2008**, *130*, 14117–14119.

(12) (a) Spies, P.; Schwendemann, S.; Lange, S.; Kehr, G.; Fröhlich, R.; Erker, G. *Angew. Chem., Int. Ed.* **2008**, *47*, 7543–7546. (b) Chase, P. A.; Jurca, T.; Stephan, D. W. *Chem. Commun.* **2008**, 1701–1703. (c) Wang, H. D.; Fröhlich, R.; Kehr, G.; Erker, G. *Chem. Commun.* **2008**, 5966–5968. (d) Axenov, K. V.; Kehr, G.; Fröhlich, R.; Erker, G. *J. Am. Chem. Soc.* **2009**, *131*, 3454–3455. (e) Jiang, C.; Blacque, O.; Berke, H. *Chem. Commun.* **2009**, 5518–5520. (f) Axenov, K. V.; Kehr, G.; Fröhlich, R.; Erker, G. *Organometallics* **2009**, *28*, 5148–5158. (g) Miller, A. J. M.; Labinger, J. A.; Bercaw, J. E. *J. Am. Chem. Soc.* **2010**, *132*, 3301–3303. (h) Geier, S. J.; Chase, P. A.; Stephan, D. W. *Chem. Commun.* **2010**, *46*, 4884–4886. (i) Ménard, G.; Stephan, D. W. *J. Am. Chem. Soc.* **2010**, *132*, 1796–1797. (j) Schwendemann, S.; Tumay, T. A.; Axenov, K. V.; Peuser, I.; Kehr, G.; Fröhlich, R.; Erker, G. *Organometallics* **2010**, *29*, 1067–1069. (k) Unverhau, K.; Lubbe, G.; Wibbeling, B.; Fröhlich, R.; Kehr, G.; Erker, G. *Organometallics* **2010**, *29*, 5320–5329.

(13) Chase, P. A.; Welch, G. C.; Jurca, T.; Stephan, D. W. *Angew. Chem., Int. Ed.* **2007**, *46*, 8050–8053.

(14) Garrett, C. E.; Prasad, K. *Adv. Synth. Catal.* **2004**, *346*, 889–900.

(15) (a) Chen, D.; Klankermayer, J. *Chem. Commun* **2008**, 2130–2131. (b) Ashley, A. E.; Thompson, A. L.; O'Hare, D. *Angew. Chem., Int. Ed.* **2009**, *48*, 9839–9843. (c) Chen, J; Venkatasubbaiah, K.; Pakkirisamy, T.; Doshi, A.; Yusupov, A.; Patel, Y.; Lalancette, R. A.; Jäkle, J. *Chem.—Eur. J.* **2010**, *16*, 8861–8867. (d) Chen, D.; Wang, Y.; Klankermayer, J. *Angew. Chem., Int. Ed.* **2010**, *49*, 9475–9478.

(16) Sumerin, V.; Chernichenko, K.; Nieger, M.; Leskelä, M.; Rieger, B.; Repo, T. *Adv. Synth. Catal.* **2011**, *353*, 2093–2110.

(17) (a) Rokob, T. A.; Hamza, A.; Stirling, A.; Soós, T.; Pápai, I. *Angew. Chem., Int. Ed.* **2008**, *47*, 2435–2438. (b) Guo, Y.; Li, S. H. *Inorg. Chem.* **2008**, *47*, 6212–6219. (c) Rajeev, R.; Sunoj, R. B. *Chem.—Eur. J.* **2009**, *15*, 12846–12855. (d) Hamza, A.; Stirling, A.; Rokob, T. A.; Pápai, I. *Int. J. Quantum Chem.* **2009**, *109*, 2416–2425. (e) Rokob, T. A.; Hamza, A.; Stirling, A.; Pápai, I. *J. Am. Chem. Soc.* **2009**, *131*, 2029–2036. (f) Privalov, T. *Dalton Trans.* **2009**, 1321–1327. (g) Pyykkö, P.; Wang, C. *Phys. Chem. Chem. Phys.* **2010**, *12*, 149–155. (h) Grimme, S.; Kruse, H.; Goerigk, L.; Erker, G. *Angew. Chem., Int. Ed.* **2010**, *49*, 1402–1405.

(18) Fan, C.; Mercier, L. G.; Piers, W. E.; Tuononen, H. M.; Parvez, M. *J. Am. Chem. Soc.* **2010**, *132*, 9604–9606.

(19) Piers, W.; Marwitz, A. J. V.; Mercier, L. G. *Inorg. Chem.* 2011No. DOI: 10.1021/ic2006474.

(20) Sumerin, V.; Schulz, F.; Nieger, M.; Leskela, M.; Repo, T.; Rieger, B. *Angew. Chem., Int. Ed.* **2008**, *47*, 6001–6003.

(21) Gábor, E.; Mehdi, H.; Pápai, I.; Rokob, T. A.; Király, P.; Tárkányi, G.; Soós, T. *Angew. Chem., Int. Ed.* **2010**, *49*, 6559–6563.

(22) The notion "hydron" is used in this text as a general term for mobile hydrogen isotopes such as the proton and the deuteron.

(23) See the Supporting Information for details.
(24) Blackwell, J. M.; Sonmor, E. R.; Scoccitti, T.; Piers, W. E. *Org. Lett.* **2000**, *2*, 3921–3923.
(25) ^{1}J-couplings between X and Y in ^{1}H and ^{2}H NMR spectra of **NXYB** are obscured by the broadness of the signals.
(26) Please see the Supporting Information for a detailed discussion on line broadening of the N*H* signal in **NHHB**.
(27) Peris, E.; Lee, J. C.; Rambo, J. R.; Eisenstein, O.; Crabtree, R. H. *J. Am. Chem. Soc.* **1995**, *117*, 3485–3491.
(28) The proton bound to N is named H1, and the hydride bound to B is assigned H8.
(29) Jiang, C.; Blacque, O.; Fox, T.; Berke, H. *Organometallics* **2011**, *30*, 2117–2124.
(30) Mason, J. *Multinuclear NMR*; Plenum Press: New York, 1987.
(31) Dziembowska, T.; Rozwadowski, Z. *Curr. Org. Chem.* **2001**, *5*, 289–313.
(32) Limbach, H.-H.; Pietrzak, M.; Sharif, S.; Tolstoy, P. M. Shenderovich, I. G.; Smirnov, S. N.; Golubev, N. S.; Denisov, G. S. *Chem.—Eur. J.* **2004**, *10*, 5195–5204.
(33) Sharif, S.; Denisov, G. S.; Toney, M. D.; Limbach, H.-H. *J. Am. Chem. Soc.* **2006**, *128*, 3375–3387.
(34) Belkova, N. V.; Ionidis, A. V.; Epstein, L. M.; Shubina, E. S.; Gruendemann, S.; Golubev, N. S.; Limbach, H.-H. *Eur. J. Inorg. Chem.* **2001**, *2001*, 1753–1761.
(35) Limbach, H.-H.; Ulrich, S.; Gründemann, S.; Buntkowsky, G.; Sabo-Etienne, S.; Chaudret, B.; Kubas, G. J.; Eckert, J. *J. Am. Chem. Soc.* **1998**, *120*, 7929–7943.
(36) Kohen, A.; Limbach, H.-H. *Isotope Effects in Chemistry and Biology*; Taylor and Francis Group: Boca Raton, FL, 2006 and references cited therein.
(37) (a) Günther, H. *NMR Spectroscopy*, 2nd ed.; John Wiley & Sons: New York, 2001. (b) Friebolin, H. *Basic One- and Two-Dimensional NMR Spectroscopy*, 3rd ed.; Wiley-VCH: Weinheim, 1998.
(38) In principle, isotope fractionation should occur where H enriches in the site exhibiting the lower ZPEs, so that the ^{1}H signals of **NHDB** and **NDHB** show different intensities. Examples of isotopic fractionation in hydrogen bonds of different strength have already been observed previously in the slow-exchange regime. Cf.: Smirnov, S. N.; Benedict, H.; Golubev, N. S.; Denisov, G. S.; Kreevoy, M. M.; Schowen, R. L.; Limbach, H.-H. *Can. J. Chem.* **1999**, *77*, 943–946.
(39) Gao, S.; Wu, W.; Mo, Y. *J. Phys. Chem. A* **2009**, *113*, 8108–8117.
(40) (a) Rendler, S.; Oestreich, M. *Angew. Chem., Int. Ed.* **2008**, *47*, 5997–6000. (b) Hog, D. T.; Oestreich, M. *Eur. J. Org. Chem.* **2009**, *29*, 5047–5056.
(41) Desiraju, G. R.; Steiner, T. *The Weak Hydrogen Bond in Structural Chemistry and Biology*; Oxford University Press: Chichester, UK, 1999.
(42) Steiner, T. *Angew. Chem., Int. Ed.* **2002**, *41*, 48–76.
(43) Klooster, W. T.; Koetzle, T. F.; Siegbahn, P. E. M.; Richardson, T. B.; Crabtree, R. H. *J. Am. Chem. Soc.* **1999**, *121*, 6337–6343.
(44) (a) Yang, J. B.; Lamsal, J.; Cai, Q.; James, W. J.; Yelon, W. B. *Appl. Phys. Lett.* **2008**, *92*, 091916. (b) Hess, N. J.; Schenter, G. K.; Hartman, M. R.; Daemen, L. L.; Proffen, T.; Kathmann, S. M.; Mundy, C. J.; Hartl, M.; Heldebrant, D. J.; Stowe, A. C.; Autrey, T. *J. Phys. Chem. A* **2009**, *113*, 5723–5735.
(45) Sumerin, V.; Schulz, F.; Nieger, M.; Atsumi, M.; Wang, C.; Leskelä, M.; Pyykkö, P.; Repo, T.; Rieger, B. *J. Organomet. Chem.* **2009**, *694*, 2654–2660.
(46) Grabowski, S. J.; Sokalski, W. A.; Leszczynski, J. *J. Phys. Chem. A* **2005**, *109*, 4331–4341.
(47) Grabowski; Grabowski, S. J.; Sokalski, W. A.; Leszczynski, J. et al. *Chem. Phys.* **2007**, *337*, 68–76. These authors state that H···H distances below 1.7 Å give strong evidence for partially covalent H···H interactions, but it has to be considered that this value is based solely on calculations on a MP2 6-311++G(d,p) level of theory.
(48) Hamilton, D. G.; Crabtree, R. H. *J. Am. Chem. Soc.* **1988**, *110*, 4126–4133.
(49) Desrosiers, P. J.; Cai, L. H.; Lin, Z. R.; Richards, R.; Halpern, J. *J. Am. Chem. Soc.* **1991**, *113*, 4173–4184.
(50) Gusev, D. G.; Nietlispach, D.; Vymenits, A. B.; Bakhmutov, V. I.; Berke, H. *Inorg. Chem.* **1993**, *32*, 3270–3276.
(51) To be able to incorporate all relevant unknowns in the fit would necessitate an unpractical number of measured data points.
(52) Bakhmutov, V. I. *Practical NMR Relaxation for Chemists*; John Wiley & Sons: Chichester, 2004.
(53) (a) Fletcher, C. M.; Jones, D. N. M.; Diamond, R.; Neuhaus, D. *J. Biomol. NMR* **1996**, *8*, 292–310. (b) Cronin, L.; Higgitt, C. L.; Perutz, R. N. *Organometallics* **2000**, *19*, 672–683. (c) Zagrovic, B.; van Gunsteren, W. F. *Proteins: Struct., Funct. Bioinf.* **2006**, *63*, 210–218.
(54) (a) Ping, F, Y. *J. Magn. Reson.* **1990**, *90*, 382–383. (b) Jones, C. R.; Butts, C. P.; Harvey, J. N. *Beilstein J. Org. Chem.* **2011**, *7*, 145–150.
(55) Stott, K.; Stonehouse, J.; Keeler, J.; Hwang, T.-L.; Shaka, A. J. *J. Am. Chem. Soc.* **1995**, *117*, 4199–4200.
(56) (a) Stott, K.; Keeler, J.; Van, Q. N.; Shaka, A. J. *J. Magn. Reson.* **1997**, *125*, 302–324. (b) Hu, H.; Krishnamurthy, K. *J. Magn. Reson.* **2006**, *182*, 173–177.
(57) The complete spectra are provided in the Supporting Information.
(58) Hadži, D.; Bratos, S. In *The Hydrogen Bond—Recent Developments in Theory and Experiments*; Schuster, P., Zundel, G., Sandorfy, C., Eds.; North-Holland Publishing Co.: Amsterdam, 1976; pp 565−611.
(59) Nibbering, E. T. J.; Elsaesser, T. *Chem. Rev.* **2004**, *104*, 1887–1914.
(60) More precisely the values should be 1.37 for ν(NH)/ν(ND) and 1.36 for ν(BH)/ν(BD) by taking the reduced masses into account.
(61) Preliminary results of PED analysis on the RI-PBE/6-31G** level of calculation show that the normal mode containing the largest component of H−H stretching in **NHHB** is 92.20 cm^{-1} (23%) and of D−D stretching in **NDDB** is 92.05 cm^{-1} (26%). All other modes in 92.20/92.05 cm^{-1} are less than 10%. A large number of vibrational modes couple and therefore the isotopic effect in frequency shift is not by a factor of $\sqrt{2}$ as would be expected.
(62) (a) Karkamkar, A.; Kathmann, S. M.; Schenter, G. K.; Heldebrant, D. J.; Hess, N.; Gutowski, M.; Autrey, T. *Chem. Mater.* **2009**, *21*, 4356–4358. (b) Bowden, M.; Heldebrant, D. J.; Karkamkar, A.; Proffen, T.; Schenter, G. K.; Autrey, T. *Chem. Commun.* **2010**, *46*, 8564–8566.
(63) (a) Lasdon, L. S.; Waren, A. D.; Jain, A.; Ratner, M. *ACM Trans. Math. Softw.* **1978**, *4*, 34–50. (b) Fylstra, D.; Lasdon, L.; Watson, J.; Waren, A. *Interfaces* **1998**, *28*, 29–55.
(64) Schegolikhin, A. N.; O.L.Lazareva, O. L. *Int. J. Vib. Spect.* **1997**, *1*, 95–116.
(65) Pedersen, B.; Frey, F.; Scherer, W. *Neutron News* **2007**, *18*, 20–22.
(66) Petricek, V.; Dusek, M.; Palatinus, L *Jana2000*; Structure Determination Software Programs: Prague, 2000.
(67) Becker, P. J.; Coppens, P. *Acta Crystallogr.* **1974**, *A30*, 129–153.
(68) (a) Perdew, J. P.; Burke, K; Ernzerhof, M. *Phys. Rev. Lett.* **1996**, *77*, 3865–3868. (b) Perdew, J. P.; Burke, K; Ernzerhof, M. *Phys. Rev. Lett.* **1997**, *78*, 1396.
(69) Yanai, T; Tew, D; Handy, D. *Chem. Phys. Lett.* **2004**, *393*, 51–57.
(70) Hariharan, P. C.; Pople, J. A. *Theoret. Chim. Acta* **1973**, *28*, 213–222.
(71) Frisch, M. J.; et al. *Gaussian 09*, Rev. A.01; Gaussian Inc.: Wallingford, CT, 2009.
(72) Jamróz, M. H. *Vibrational Energy Distribution Analysis*, VEDA 4.0; Warsaw, 2004.